E3S Web of Conferences **383**, 04005 (2023) https://doi.org/10.1051/e3sconf/202338304005
TT21C-2023

Traction SRM simulation taking into account the radial interaction of the rotor and stator

Maxim Tchavychalov[1*], *Natalya* Yaitskova[1]

[1]Rostov State Transport University, 2, Rostovskogo Strelkovogo Polka Narodnogo Opolcheniya sq., Rostov-on-Don, 344038, Russia

Abstract. The article presents the features of traction switched reluctance motors with a diametric closure of the magnetic flux and a “short field”. A computer simulation of a motor with a short field is performed for the ideal location of the rotor inside the stator, as well as for two cases of rotor displacement. The hodographs of the radial interaction forces of the rotor and stator are calculated.

1 Introduction

One of the main guidelines for the innovative development of transport systems is the replacement of equipment with expired service life with new equipment with high technical and economic indicators.

New vehicles must have high reliability, energy efficiency, and at the same time comfort for passengers and staff is an important factor. The world's leading scientists note that technologies whose main trend was "bigger, faster, higher" have now been replaced by new technologies whose trend has become "better, safer, quieter".

One of the main directions for improving the operational performance of transport systems is the use of a brushless traction drive. Currently, traction drive with asynchronous motors is becoming increasingly widespread in our country. However, the search for a more advanced engine for transport systems continues. The switched reluctance motors (SRM) have good prospects – the simplest in design among the closest competitors.

The theory of the SRM and the drive based on it is intensively developing, thanks to this, according to the main technical and economic indicators, the SRM is on a par with the best examples of traditional electric machines with a circular field in the air gap.

Noise and vibrations accompany almost any type of transport. The sources of the increased noise level are the mechanical energy converter (gearbox), the propulsion of the transport system (wheel-rail interaction, wheel-road surface, etc.), as well as auxiliary systems, for example, fans of cooling systems. A traction SRM is also a source of noise, regardless of its type. Any electric machine is characterized by noise from the effects of radial forces of attraction of the rotor to the stator, magnetostriction, aerodynamic noise, etc.

* Corresponding author: chavychalov-maxim@yandex.ru

2 Causes of SRM noise

As in other electric machines, radial forces of attraction between the stator and the rotor act in the SRM, leading to vibrations and, as a consequence, acoustic noise. Radial forces arise as a result of the excitation of phase windings and can be considered a disturbing force of stator vibrations [1]. The frequency of phase excitation is defined as

$$f_p = \frac{\omega}{2\pi} \cdot P_r, \quad (1)$$

where ω is the rotor rotation frequency, P_r is the number of teeth of the rotor.

The vibration level is maximum when any of the frequencies

$$f_n = n \cdot f_p, n = 1,3,5,7... \quad (2)$$

coincides with the natural frequency of the stator f [2]. When the even harmonics of the disturbance coincide with the natural frequency of the SRM design, the vibration level decreases. Therefore, to reduce the noise level of the SRM, the natural frequency of the SRM must be known. Its value can be obtained using the finite element method or an analytical expression [2].

When deriving the analytical formula for determining the natural frequency of the stator, it is assumed that the stator magnetic core package is a cylindrical shell with a thickness of b_{sy} (the height of the stator back) and a length of L. When a vertical load w is applied to the annular structure, the resulting deformation tends to change the structure to an elliptical shape. The potential energy resulting from the impact of the load must be equal to the kinetic energy resulting from deformation. The circular natural frequency can be defined as

$$\omega^2 = \frac{2}{12\pi(1-\gamma^2)\left(\frac{\pi}{4}-\frac{2}{\pi}\right)} \cdot \frac{E}{\rho} \cdot \frac{b_{sy}^2}{r_y^4}, \quad (3)$$

where γ is the Poisson's ratio, p is the density of the material, r_y is the average radius of the stator shell, defined as

$$r_y = \frac{D_o - b_{sy}}{2}, \quad (4)$$

where D_o is the outer diameter of the stator package.

It can be seen from the above equations that the natural frequency can be changed to a greater extent by selecting the height of the stator back, since the outer diameter of the package is usually set for the required values of power and rotor speed. It follows from this that the thickness of the stator back is a design parameter when determining the natural frequency. It is recommended to design the machine in such a way that its natural frequency is as high as possible to avoid resonance at high excitation frequencies. It should be borne in mind that with an increase in the thickness of the stator back, the weight of the SRM increases, the space under the stator windings decreases, i.e. to achieve the required output parameters, the current density in the conductors will have to be increased, which negatively affects losses in copper. In addition, when the b_{sy} value increases, the specific power of the machine decreases. As a rational value of the thickness of the stator back, such is taken that the flow coupling in it is equal to half the value of the flow coupling in the stator tooth. This reduces losses in the magnetic circuit, which is especially important at high rotational speeds.

The expression for determining the natural frequency of the stator is based on the assumption that the stator and the outer housing are an entire ring. However, this assumption is not always valid. For machines with a ratio of the stator length to its radius of more than

https://doi.org/10.1051/e3sconf/202338304005

0.2, a different approach is required. In [3], an equation is given for determining the natural frequency of the stator, based on the energy method and the Rayleigh-Ritz principle, taking into account the following structural elements of the SRM: housing, back and teeth of the stator, coils of windings and ventilation openings. The influence of coils and their impregnation on the occurrence of resonance is considered in [4]. In [5], a method for calculating the natural frequencies of the SRM design is proposed, based on the energy method similar to asynchronous machines. The authors also demonstrate the effect of changes in the arc of the teeth and coil parameters on the value of the natural frequency of the stator. As a rule, neglecting the coils when calculating the natural frequency of the stator eventually gives an error of about 20-30%.

Radial forces acting on the rotor are the most significant source of noise in the SRM [6]. When the rotor is displaced and an imbalance occurs, the level of radial forces, and, consequently, noise, increases significantly and can lead to breakdowns and failures of the SRM [7, 8]. In this case, the frequency of the disturbing effect is defined as

$$f_{\mathrm{d}} = \frac{n \cdot i}{60} \quad (5)$$

where i is a positive integer.

3 SRM mathematical model

Since SRM is currently a fairly popular research topic, experts have described various design options for both the machine itself and the converter necessary for its effective operation. In this paper, the simulation of the SRM is carried out taking into account the power supply of its phase windings from a semiconductor converter according to the "asymmetric bridge" scheme. This scheme allows you to provide most control algorithms and is relatively easy to implement in practice. Assuming that the phase windings are identical, the mathematical model is based on the example of one phase of the SRM. An equivalent substitution scheme for this case is shown in Fig. 1.

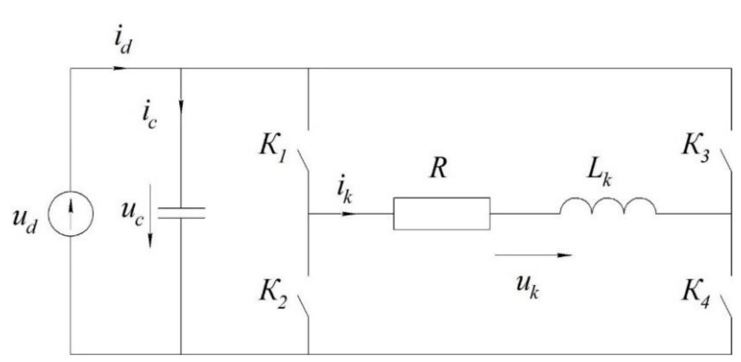

Fig. 1. SRM phase replacement scheme.

In the mathematical description of the SRM, it is necessary to take into account the path of the main magnetic flux. On this basis, it is possible to distinguish the configurations of the SRM with a diametric closure of the magnetic flux (Fig. 2a) and the SRM with the so-called "short field" ("short flux SRM") (Fig. 2b).

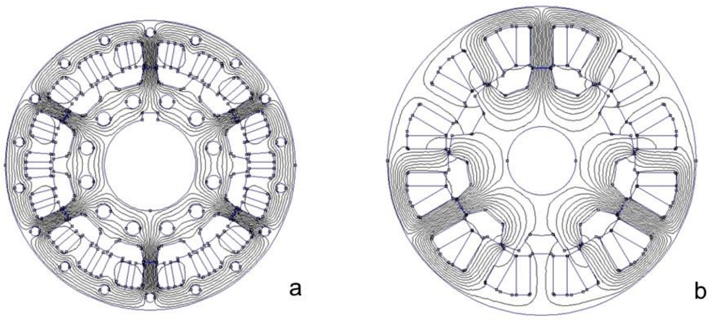

Fig. 2. Examples of SRM configurations with diametrically closed magnetic flux (a) and "short field" (b).

When simulating a SRM with a diametric closure of the magnetic flux, the following assumptions are made:

- the mutual inductance of the phases is zero;
- steel losses and mechanical losses are not taken into account;

The keys are considered ideal, i.e. they perform switching without time delays and voltage drops on them.

Then the Kirchhoff equation can be compiled for the SRM phase

$$u_c = i_a \cdot R + \frac{d\psi_a}{dt}, \quad (6)$$

where u_c is the voltage applied to the phase; i_a – phase current; R is the resistance of the phase winding; ψ_a – flow coupling of the phase winding; t – time.

The flow coupling of the phase windings is a function of the flowing current *i* and the angle of rotation of the rotor θ (Fig. 3). In Fig. 3, the angle of rotor position is indicated by θ_a, corresponding to the aligned position of the rotor (the rotor tooth is located opposite the stator tooth), θ_u – to the unaligned position (the stator tooth is opposite the rotor slot).

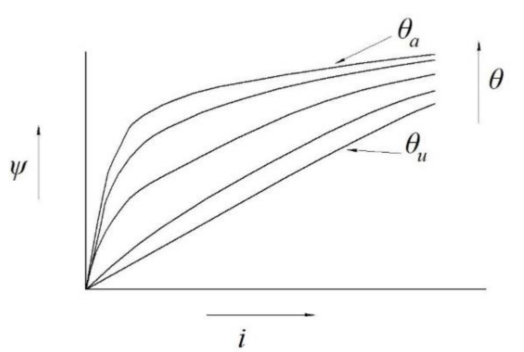

Fig. 3. Dependence $\psi_a=f(i_a, \theta)$.

As a result, we get

$$u_c = i_a \cdot R + \frac{d\psi_a(i,\theta)}{dt} = i_a \cdot R + \frac{\partial\psi_a(i_a,\theta)}{\partial i_a} \cdot \frac{di_a}{dt} + \frac{\partial\psi_a(i_a,\theta)}{\partial\theta} \cdot \omega \quad (7)$$

Where $\frac{\partial\psi_a(i_a,\theta)}{\partial i_a}$ is the differential inductance; $\frac{\partial\psi_a(i_a,\theta)}{\partial\theta}$ – EMF coefficient; ω is the rotation frequency of the rotor.

By reducing equation 7 to the Cauchy form we obtain

$$\frac{di_a}{dt} = \frac{1}{\frac{\partial \psi_a(i_a,\theta)}{\partial i_a}} \cdot \left(u_c - i_a \cdot R - \frac{\partial \psi_a(i_a,\theta)}{\partial \theta} \cdot \omega\right). \quad (8)$$

Thus, for an *N*-phase SRM, the windings of which are connected according to the scheme shown in Fig. 1, it is possible to write a system of differential equations 9

$$\begin{cases} \frac{di_k}{dt} = \frac{1}{\frac{\partial \psi_k(i_k,\theta)}{\partial i_k}} \cdot \left(u_c - i_k \cdot R - \frac{\partial \psi_k(i_k,\theta)}{\partial \theta} \cdot \omega\right), k = 1,2,\ldots,N; \\ \frac{du_c}{dt} = \frac{i_c}{C}, \\ i_s = i_c + \sum_{k=1}^{N} i_k . \end{cases} \quad (9)$$

When mathematically describing a SRM with a "short field", it is necessary to take into account the mutual inductance of the phase windings. In this case, phase flow coupling is considered as

$$\psi_1 = f(i_1, i_2, \ldots, i_N, \theta). \quad (10)$$

For the *N*-phase SRM, when the flow coupling derivative is disclosed, the equation 7 is similar to

$$u_c = i_k \cdot R + \frac{\partial \psi_k(i_1,i_2,\ldots,i_N,\theta)}{\partial i_1} \cdot \frac{di_1}{dt} + \frac{\partial \psi_k(i_1,i_2,\ldots,i_N,\theta)}{\partial i_2} \cdot \frac{di_2}{dt} + \cdots$$
$$\ldots + \frac{\partial \psi_1(i_1,i_2,\ldots,i_N,\theta)}{\partial i_N} \cdot \frac{di_3}{dt} + \frac{\partial \psi_k(i_1,i_2,\ldots,i_N,\theta)}{\partial \theta} \cdot \omega,$$
$$k = 1,2,\ldots,N. \quad (11)$$

The numerical solution of the system of equations 11 on a computer is complicated by the presence of algebraic loops. In this case, the calculation can be performed by iterative methods. A simpler and faster way to calculate the characteristics of a SRM with a "short field" is to transform the source data. So, the dependence 11 necessary for the calculation must be converted to

$$i_1 = f(\psi_1, i_2, \ldots, i_N, \theta) \quad (12)$$

Then, for a SRM with a "short field", we can write a system of equations

$$\begin{cases} \psi_k = \int (u_c - i_k \cdot R) dt, \\ i_k = f(\psi_k, i_j, \theta), \\ \frac{du_c}{dt} = \frac{i_c}{C}, \end{cases} \quad (13)$$
$$k = 1,2,\ldots,N,$$
$$j = 1,2,\ldots N, j \neq k.$$

It is known that the following forces act on the SRM rotor: normal F_n, tangential F_τ, and lateral F_l [9]. The direction of action of these forces is indicated in Fig. 4.

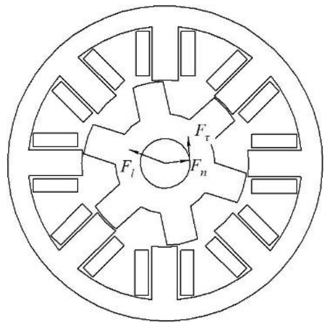

Fig. 4. Direction of forces acting on the SRM rotor.

For the mathematical description of the force action on the rotor, phase flow coupling is considered as

$$\psi = f(i, \theta, l_\delta, l_r) \tag{14}$$

where l is the value of the air gap; l_r is the length of the rotor.

The electromagnetic torque is defined as

$$T(i, \theta, l_\delta, l_r) = \frac{\partial W'(i,\theta,l_\delta,l_r)}{\partial \theta}, \tag{15}$$

where W' is the co-energy, defined as

$$W'(i, \theta, l_\delta, l_r) = \int \psi(i, \theta, l_\delta, l_r)\, di. \tag{16}$$

Usually, the electromagnetic moment is considered as a function of the phase current and the angle of rotation of the rotor $T(i, \theta)$.

The tangential force is defined as follows

$$F_\tau(i, \theta, l_\delta, l_r) = \frac{T(i,\theta,l_\delta,l_r)}{R_r} \tag{17}$$

where R_r is the radius of the rotor.

The normal and lateral forces are determined respectively

$$F_n(i, \theta, l_\delta, l_r) = \frac{\partial W'(i,\theta,l_\delta,l_r)}{\partial l_\delta}, \tag{18}$$

$$F_l(i, \theta, l_\delta, l_r) = \frac{\partial W'(i,\theta,l_\delta,l_r)}{\partial l_r}. \tag{19}$$

Considering the mechanical interaction with the external system, we assume that the SRM shaft is coupled to the shaft of the mechanism absolutely rigidly. In this case, the mechanical system can be represented in the form of Fig. 5.

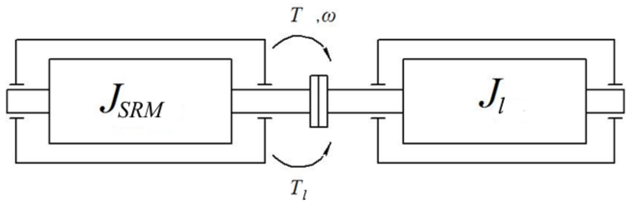

Fig. 5. Kinematic scheme "SRM-external mechanism".

Knowing the moment of inertia of the rotor SRM J_{SRM} and the moment of inertia of the external mechanism J_l in this case, it is possible to determine the reduced moment of inertia of the system J' and write down the equation of motion

$$J'\frac{d\omega}{dt} = T - T_l - B \cdot \omega, \qquad (20)$$

where T_l is the moment of resistance; B is a coefficient that takes into account the friction in the bearing assemblies and the friction against the air.

The torque of the SRM is produced by each phase, therefore it can be defined as

$$T = \sum_{k=1}^{N} T_k(i, \theta, l_\delta, l_r) \qquad (21)$$

Thus, equation 20 in the Cauchy form takes the form

$$\frac{d\omega}{dt} = \frac{1}{J_{пр}}\left(\sum_{k=1}^{N} T_k(i, \theta, l_\delta, l_r) - T_с - B \cdot \omega\right) \qquad (22)$$

Computer model is realized in MATLAB/Simulink and shown at Fig. 6. The model consists of 3 parts. The electrical part simulates the operation of the converter according to the scheme of an asymmetric bridge with ideal semiconductor elements and a power source. In the blocks Phase1, Phase2 and Phase 3, the above equations of the electric balance of the phase are solved using a single lookup table. In the mechanical part, the above equation of motion of the electric drive is solved, and the current angular position of the rotor is determined. In the control part, based on the angular position of the rotor and the value of the phase currents, signals are generated that are fed to the converter transistors.

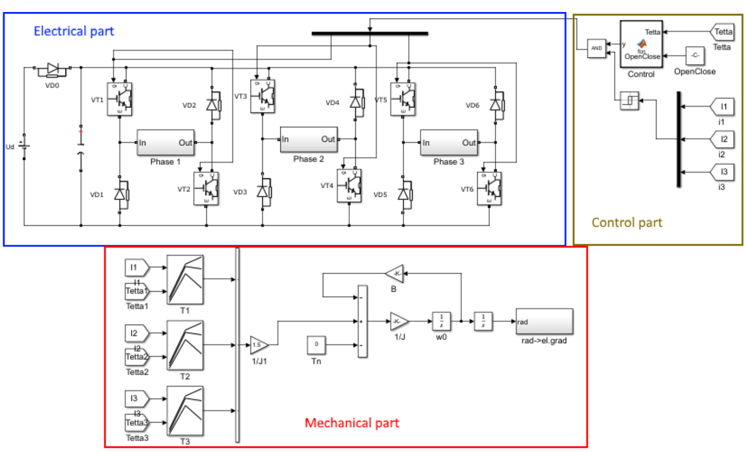

Fig. 6. Matlab/Simulink model.

4 Results of simulation

The simulation is carried out by a switched reluctance motor of an elevator mechanism. The patterns of magnetic flux SRM is shown in Fig. 7. Results of phase current calculation are shown in Fig. 8.

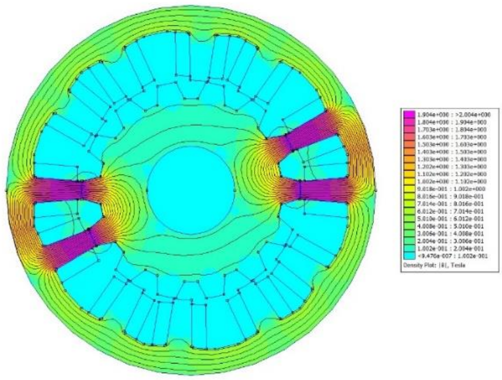

Fig. 7. Magnetic field of the traction motor of the elevator mechanism.

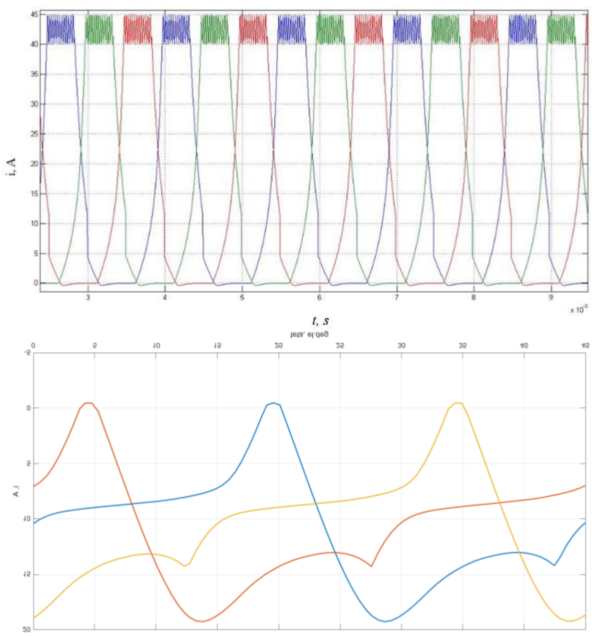

Fig. 8. Dependence i(θ)

When studying the radial interaction of the rotor and the stator, two cases are considered: the shift of the axis of rotor rotation (case 1) and the shift of the rotor relative to the axis of rotation (case 2). The value of the shift in both cases is assumed to be 10% of the value of the air gap along the X and Y axes. Since the coils of the phase windings are connected in series, a change in the magnetic resistance under the stator teeth in the case of a rotor shift will not affect the value of the phase current. The values of the phase currents and the angle of rotor rotation obtained above are used in the FEMM software to calculate radial forces from the Maxwell stress tensor. As a result, for each of the cases, the values of the radial force along the orthogonal axes are obtained. However, a more detailed picture is given by the hodograph of the vector of the total radial force acting on the rotor during motor operation [10] (Fig. 9-11).

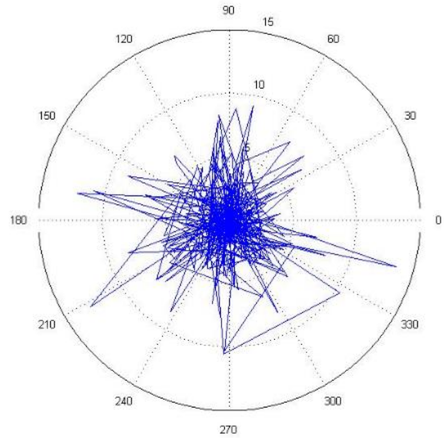

Fig. 9. Radial force hodograph of balanced SRM.

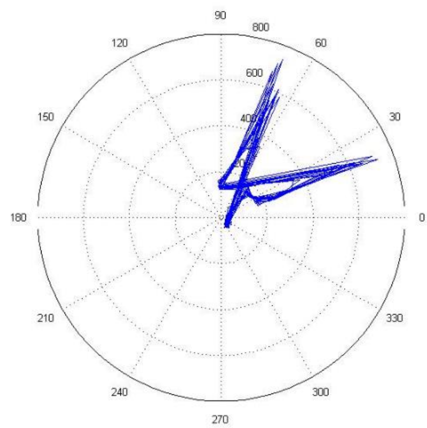

Fig. 10. Radial force hodograph of unbalanced SRM (case 1).

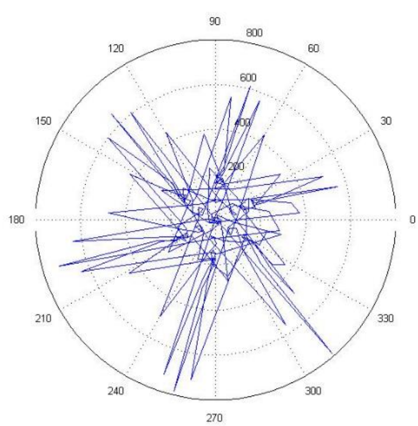

Fig. 11. Radial force hodograph of unbalanced SRM (case 2).

5 Conclusion

As can be seen from the simulation results, the radial displacement of the rotor significantly increases the level of radial forces. This will help to increase the level of acoustic noise and vibration. At the same time, in “short field” SRM, when the windings of one phase are connected in parallel, in the case of displacement of the rotor, feedback begins to act in the form of a force tending to return the rotor to the central position, as can be seen from the simulation results. Thus, the radial shift of the rotor of SRM with parallel connection of windings will have less effect on the occurrence of noise and vibrations compared to motors with diametrically closed magnetic flux.

References

1. M. Ehsani, G. Yimin, A. Emadi, CRC Press (2009)
2. R.S. Colby, F.M. Mottier, T.J.E. Miller, IEEE Transactions on Industry Applications **32** (1996)
3. R.S. Girgis, S.P. Verma, IEEE Transactions on Electrical Power Apparatus B. **128** (1981)
4. R.K. Singal, K. Williams, S.P. Verma, Experimental Mechanics **30** (1990)
5. C. Yongxiao, W. Jianhua, H. Jun, *Analytical calculation of natural frequencies of stator of switched reluctance motor,* in 8th International Conference on Electrical Machines and Drives (1997)
6. J.O. Fielder, K.A. Kasper, F. Chaparro R.W. De Donker, IEEE Industry applications conference (2006)
7. T.J.E. Miller, IEEE Transactions on industry applications **31** (1995)
8. L. Szabo, M. Ruba, IEEE Eurocon transactions (2010)
9. M. Divandary, A. Dadpour, *Radial force and torque ripple optimization for acoustic noise reduction of SRM drives via fuzzy logic control, in Industry applications (INDUSCON),* 9th IEEE/IAS International Cobnference on (2010)
10. R. Karthikeyan, K. Vijayakumar, R. Arumugam, International journal of computer applications **6** (2010)